Eur Biophys J (1999) 28: 133–141

ARTICLE

Andrew H. A. Clayton · William H. Sawyer

The structure and orientation of class-A amphipathic peptides on a phospholipid bilayer surface

Received: 8 April 1998 / Revised version: 6 July 1998 / Accepted: 7 August 1998

Abstract The amphipathic α-helix is a recognised structural motif that is shared by membrane-associating proteins and peptides of diverse function. The aim of this paper is to determine the orientation of an α-helical amphipathic peptide on the bilayer surface. We use five amphipathic 18-residue peptide analogues of a class A amphipathic peptide that is known to associate with a bilayer surface. Tyrosine and tryptophan are used as spectroscopic probes to sense local environments in the peptide in solution and when bound to the surface of unilamellar phosphatidylcholine vesicles. In a series of peptides, tryptophan is moved progressively along the sequence from the nonpolar face (positions 3, 7, 4) to the polar face of the peptide (positions 2, 12). The local environment of the tryptophan residue at each position is determined using fluorescence spectroscopy employing quantum yield, and the wavelength of the emission maximum as indicators of micropolarity. The exposure of the tryptophan residues at each site is assessed by acrylamide quenching. On association with vesicles, the tryptophan residues at positions 3, 7 and 14 are in nonpolar water-shielded environments, and the tryptophan at position 12 is in an exposed polar environment. The tryptophan at position 2, which is located near the bilayer-water interface, exhibits intermediate behaviour. Analysis of the second-derivative absorption spectrum confirmed that the tyrosine residue at position 7 is in a nonpolar water-shielded environment in the peptide-lipid complex. We conclude that these class A amphipathic peptides lie parallel to the lipid surface and penetrate no deeper than the ester linkages of the phospholipids.

Key words Amphipathic helix · Lipid-protein interactions · Fluorescence spectroscopy · Second-derivative absorption spectroscopy

A. H. A. Clayton · W. H. Sawyer (✉)
The Russell Grimwade School of Biochemistry and Molecular Biology, The University of Melbourne, Parkville, Victoria 3052, Australia
e-mail: w.sawyer@biochemistry.unimelb.edu.au

Introduction

An amphipathic α-helix has opposing polar and nonpolar faces along its helical axis. It is a common structural motif in lipid-associating polypeptides including transmembrane proteins and certain polypeptide venoms, hormones and antibiotics. Certain peptides that exist in a disordered conformation in aqueous solvents are believed to adopt an amphipathic α-helical conformation on association with lipid surfaces. The lipid surface may be a phospholipid bilayer or, in the case of lipoproteins, a phospholipid monolayer which encloses a core of neutral lipid. It is generally assumed that an amphipathic helix orients on a lipid surface with its hydrophobic face directed towards the lipid structure and the polar face directed towards the aqueous phase.

Several theoretical models attempt to predict the orientation of the amphipathic helix on a lipid surface based on structural and physico-chemical parameters of the peptide and phospholipid lipid bilayer. Eisenberg et al. (1989) suggested that the hydrophobic moment of the α-helix and its average hydrophobicity could be used to classify helices into transmembrane, lipid-surface and protein-surface categories. Segrest et al. (1990) classified amphipathic helices into seven distinct classes based on inferred physicochemical and structural properties derived from model building. Brasseur (1991) classified lipid-associating helices according to the angles defined by a sector formed by hydrophobic and hydrophilic residues when the helix is represented as a helical wheel. In this classification, an α-helix with a hydrophobic sector angle greater than 180° should be capable of self-association in the membrane to form a transmembrane pore. If the sector angle is 180° the helix should lie parallel to the membrane surface, and if it is less than 180° it should stabilise the edge of discoidal bilayer structures. The importance of such considerations becomes apparent when it is realised that the amphipathic α-helix is the main structural entity which guides the association of apolipoproteins with lipid emulsions.

Model de novo designed peptides, which bear no resemblance to sequences found in apolipoproteins but contain the essential features expected of lipid binding helices, have been studied in several laboratories. These studies have examined factors such as peptide hydrophobicity, hydrophobic face sector angle (De Kroon et al. 1990; Kiyota et al. 1996), charge topography (Kanellis et al. 1980; De Kroon et al. 1990; Mishra and Palgunachari 1996), helix macrodipole effects (Venkatachalapathi et al. 1993) and the effect of dual tandem repeats and specific amino acid replacements on the lipid-peptide interaction (Mishra et al. 1994, 1995). Some workers have correlated these properties with cytolytic and antimicrobial activities (Dathe et al. 1996; Kiyota et al. 1996).

Interpretation of these experiments is based on the implicit assumption that an amphipathic α-helix orients parallel to the lipid surface with the nonpolar face of the helix directed towards the lipid phase and the polar face towards the polar phase. However, there is little direct experimental evidence for or against this model. The few crystal structures of membrane proteins that are currently available cannot answer this question as they refer to integral membrane proteins that possess transmembrane helices. Solid state NMR measurements, attenuated total reflection infrared spectroscopy and circular dichroism measurements of peptides associated with oriented phospholipid multilayers are capable of distinguishing between transmembrane and surface helices (Vogel 1987; Brasseur et al. 1990; Hefele et al. 1990; Wu et al. 1990; Huang and Wu 1991; Shon et al. 1991). However, the orientation of peptides studied to date appears to be sensitive to peptide surface density and to the physical state of the lipid (acyl chain saturation, bilayer hydration and phase state).

The aim of the present work is to test experimentally the assumption that class A amphipathic helices orient parallel to the membrane surface. We make use of a set of 18-residue amphipathic peptides each containing two intrinsic spectroscopic probes, namely, a single tryptophan residue whose fluorescence properties can be used to determine the rotational dynamics of the indole side chain and the polarity of its local environment, and a single tyrosine residue whose absorption properties can also be used to sense the polarity of its environment. We report on the design, synthesis and spectral characterisation of these peptides and determine if the results support the parallel surface orientation model or a transmembrane model of the peptide-lipid complex.

Materials and methods

Materials

Synthesis grade protected amino acids were purchased from Auspep and were used as received. Other reagents used in peptide synthesis were reagent grade. Egg lecithin phosphatidylcholine (eggPC) was received as a chloroform-methanol stock solution from Lipid Products (UK) and used without further purification. Methanol was HPLC grade (British Drug Houses). All buffers were prepared using Milli-Q distilled water.

General methods

Peptides were synthesised by the solid phase method using standard Fmoc chemistry and an Applied Biosystems Peptide Synthesizer (Model 441A). The crude peptides were purified by reversed phase HPLC (Applied Biosystems solvent delivery and diode array detection) using a Brownlee column (Aquapore ODS 20 μm, 250×10 mm). The mobile phase consisted of a gradient of acetonitrile-water (0.1% trifluoroacetic acid). The identity of the peptides was confirmed by matrix-assisted laser desorption and ionisation time-of-flight mass spectrometry (MALDI-TOF). Peptide concentrations (10 mM Tris, 150 mM NaCl, pH 7.4) were determined from the peptide absorption spectra using a molar extinction coefficient at 280 nm of 6970 M^{-1} cm^{-1} for peptides A, B, D and E and 5690 M^{-1} cm^{-1} for peptide C. EggPC vesicles (20–24 nm diameter) were prepared by sonication according to established procedures (New 1990).

Spectroscopic measurements

Second-derivative absorption spectra were recorded using a Carey 5 UV-Vis spectrometer in second-derivative mode with an integration time of 1 s, a bandwidth of 2 nm and a data interval of 1 nm. The molar ratio of peptide to lipid was 1:100 (20 μM peptide). Spectra were corrected for incomplete binding of the peptide to lipid.

Fluorescence measurements were made with a SPEX Fluorolog τ2 frequency domain fluorometer equipped with a 450 W Xe lamp light source. For steady-state measurements, excitation was with vertically polarised light with the emission polariser set at 54.7° to eliminate polarisation artifacts and to reduce contributions from vesicle scattering. Excitation at 295 nm was used to preferentially excite tryptophan. Baseline fluorescence spectra were first recorded from a lipid blank containing 1.33 mM eggPC unilamellar vesicles. A small aliquot (< 50 μl) of concentrated peptide solution was then added to the cuvette to give a total peptide concentration of 1 μM, corresponding to a peptide : lipid ratio of 1:1300. The solution was mixed and equilibrated for 15 min before measurement of the fluorescence spectrum. No time dependence was observed over a period of 1 h. After subtraction of the appropriate blank, the fluorescence maximum was determined from the wavelength at which the first derivative was zero. Steady-state anisotropies (r) were calculated according to: $r = (I_v - GI_h)/(I_v + 2GI_h)$, where G is the grating correction factor, and I_v and I_h are the intensities of the vertically and horizontally polarised components of the emission (λ_{ex}, 295 nm; λ_{wm}, 350 nm; slits, 3.8 nm).

Circular dichroism (CD) measurements were made at 20 °C using an AVIV 62DS spectrometer and a 1 mm path-

length quartz cuvette. Sample concentrations and molar ratios of peptide to lipid were the same as for the fluorescence measurements. For each sample, 30 measurements were averaged (integration time, 5 s/measurement). Corrections for background contributions to the ellipticity were made by subtraction of an appropriate vesicle or buffer blank.

Quenching with acrylamide and 5-doxyl stearate

Acrylamide quenching was performed using excitation at 295 nm to excite tryptophan preferentially and to reduce absorption due to acrylamide. Small aliquots of an acrylamide stock solution (4 M) were added to the peptide-lipid suspension (mole ratio, 1:1300), and the fluorescence intensity recorded at 360 nm. Intensities were corrected for dilution and scatter. Quenching data were analysed according to the Stern-Volmer relationship:

$$F_0/F = 1 + k_q \tau [Q]$$

where F and F_0 are the corrected fluorescence intensities in the presence and absence of the quencher (Q), respectively, τ is the average fluorescence lifetime, and k_q is the apparent bimolecular rate constant which also reflects the exposure of the fluorophore to the quencher.

Quenching with 5-doxyl stearate was performed by adding aliquots of a stock solution (2 mM) to a suspension of each peptide-lipid complex and allowing equilibration for 2 h. The relative efficiency of quenching is expressed as $(F_0/F) - 1$.

Results

Peptide design

The sequences shown in Fig. 1 and Table 1 are based on a class A amphipathic peptide which is known to associate with a phospholipid bilayer surface (Venkatachalapathi et al. 1993). This peptide, referred here as peptide A, competes with Apo A–I for sites on a phospholipid surface, and mimics Apo A–I in the activation of lecithin:cholesterol acyl transferase (Venkatachalapathi et al. 1993). Peptides A, B, D and E have a single tyrosine residue at position 7 whose local environment can be probed using second-derivative absorption spectroscopy (Ragone et al. 1984). In addition, each peptide contains a single tryptophan residue at a unique position along the sequence to act as an intrinsic fluorescence probe of the structure of the peptide-lipid complex. Note that the tryptophan is progressively moved from position 2 in peptide A, to position 3 in B, position 7 in C, position 12 in D and position 14 in E. The use of single tryptophan peptides affords a method of determining the orientation of the helix on the lipid surface. In adopting an α-helical conformation, the 18-residue peptides would possess five complete helical turns. As shown by the helical wheel representation in Fig. 1, positions 3, 7 and 14 should be located centrally in the nonpolar face of the helix, position 12 in the middle of the polar face, and position 2 near the polar-nonpolar boundary. If the amphipathic helix lies parallel to the lipid-water interface, the fluorescence from the tryptophan residues at positions 3, 7 and 14 should be determined by the hydrophobic, water-shielded environment provided by the lipid phase, whilst the fluorescence of tryptophan at position 12 should be determined by the polar environment provided by the aqueous phase; the characteristics of tryptophan at position 2 should be intermediate between the two.

An important consideration is whether the substitution at particular positions along the sequence radically perturbs the amphipathic nature of the α-helix. The average hydrophobic moments of the peptides are shown in Table 1. Except for the slightly higher average hydrophobicities of peptide A and D owing to the substitution of a tryptophan by a charged amino acid, the values are not greatly affected by the position of the tryptophan residue. Values of the re-

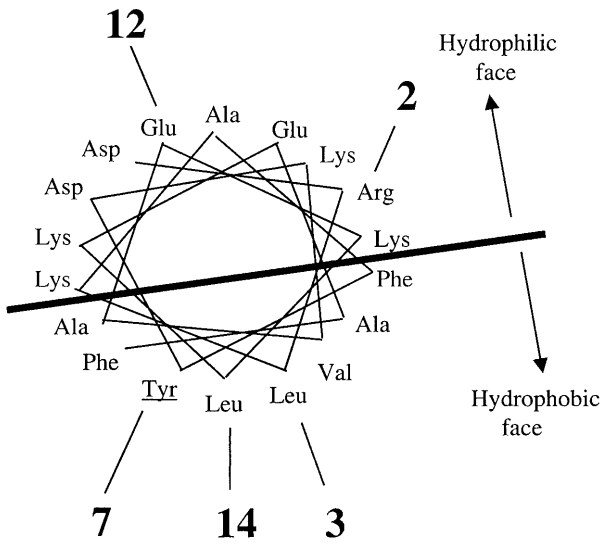

Fig. 1 Helical wheel representation of 18-residue amphipathic peptides. The figures in *bold* refer to the positions of tryptophan substitution in peptides A, B, C, D and E. The single tyrosine at position 7 is *underlined*. The *solid line* represents the boundary between the hydrophilic and hydrophobic faces of the α-helix

Table 1 Calculated average hydrophobicity ($\langle H \rangle$) and average hydrophobic moment ($\langle \mu_H \rangle$) of the 18-residue amphipathic peptides together with HPLC retention time data

Peptide (Trp position)	Sequence	$\langle \mu_H \rangle$	$\langle H \rangle$[a]	HPLC retention time (±0.2 min)
A (2)	D**W**LKAFYDKVAEKLKEAF	0.484	−0.043	33.7
B (3)	DR**W**KAFYDKVAEKLKEAF	0.515	−0.242	28.2
C (7)	DRLKAF**W**DKVAEKLKEAF	0.556	−0.198	30.9
D (12)	DRLKAFYDKVA**W**KLKEAF	0.445	−0.142	26.4
E (14)	DRLKAFYDKVAEK**W**KEAF	0.514	−0.242	25.7

[a] Calculated using the normalised hydrophobicities for amino acid side chains list by Eisenberg et al. (1989)

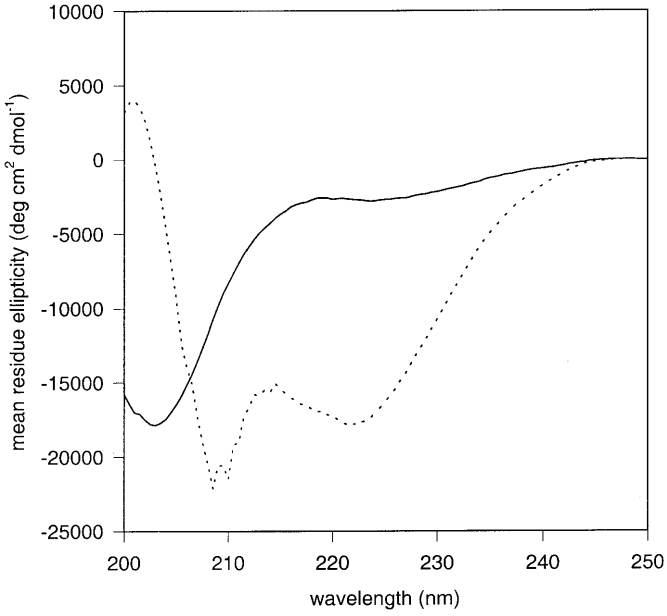

Fig. 2 Circular dichroism spectra of peptide A at 20 °C in solution (*solid line*) and complexed to eggPC vesicles (*dashed line*) (peptide : lipid mole ratio, 1 : 1300). The spectra are also representative of peptides B, D and E

verse phase HPLC retention times indicate that hydrophobic interactions between the peptide and the stationary phase of the column are not related to values of the average hydrophobicity or hydrophobic moment or to whether the tryptophan is located on the polar or nonpolar face of the helix (Table 1).

The question of whether substitution by tryptophan perturbs the secondary structure of the peptides was assessed by CD measurements. In solution, the mean elliptically at 222 nm of peptides A–E was -2766 ± 542 (SD) deg cm^2 dmol^{-1}. In the lipid-peptide complexes (mole ratio peptide : lipid, 1 : 1300) the ellipticities decreased to an average value of $-18\,293 \pm 475$ (SD) deg cm^2 dmol^{-1} for peptides A, B, D and E, indicating that the formation of α-helix was not substantially dependant on the tryptophan position in these peptides. Figure 2 illustrates this change for peptide A. Peptide C had a higher ellipticity ($-13\,176$ deg cm^2 dmol^{-1}) which resulted from substitution of tyrosine by tryptophan near the centre of the sequence. These values are generally higher than the value of $-25\,000$ deg cm^2 dmol^{-1} found for a similar N- and C-terminally blocked (18A) peptide (Mishra et al. 1994) complexed with dimyristoylphosphatidylcholine. However, the blocked 18A peptide was shown to self-associate at high concentrations, causing a decrease in mean residue ellipticity to $-25\,000$ deg cm^2 dmol^{-1} *in the absence of lipid* (Venkatachalapathi et al. 1993). The higher helicity values reported for the blocked peptide could result from decreased fraying of the termini or from peptide-peptide interactions, a self-association that is undesirable from the point of view of the present experiments. We also note that application of the usual rules for determining the helicity of proteins cannot be applied to small peptides owing to significant contributions of the aromatic amino acids to the far-UV CD (Chakrabartty et al. 1993). In particular, tyrosine and phenylalanine make positive contributions to the ellipticity at 222 nm, thereby causing the percent α-helix to be underestimated. Tryptophan can either have a positive or negative contribution to the far-UV CD (Adler et al. 1973). A more appropriate measure of helicity is to compare the mean residue ellipticities of the present peptide-lipid complexes with other α-helical peptides used in tryptophan fluorescence footprinting studies. The values for α-helical calmodulin-binding peptides ($-12\,900$ to $-24\,000$ deg cm^2 dmol^{-1}; O'Neil et al. 1987) and for α-helical ion-channel peptides ($-18\,990$ to $-22\,650$ deg cm^2 dmol^{-1}; Chung et al. 1992) are within the range for the present peptide-lipid complexes.

Table 2 *R* parameters[a] determined from the second-derivative absorption spectra for the 18-residue amphipathic peptides in buffer and when bound to egg phosphatidylcholine bilayer vesicles (100 : 1 molar ratio lipid : peptide)

Peptide (sequence position)	Tyrosine sequence position	*R* values[a] (±0.05)	
		Buffer	Vesicles
A (2)	7	0.94	0.58
B (3)	7	0.94	0.49
C (7)	No tyrosine	0.70	0.64
D (12)	7	0.83	0.45
E (14)	7	0.88	0.48

[a] The *R* value is the ratio if the peak-to-peak distances in the second-derivative spectrum between the minimum at 283 nm and the maximum at 287 nm, and the minimum at 290.5 nm and the maximum at 295 nm (Ragone et al. 1984)

The fluorescence experiments to be described were conducted at high lipid : peptide molar ratios (1300 : 1) to ensure that all the peptide was bound and that free peptide did not contribute to the spectroscopic signal. The lipid to peptide ratio at which all peptide was bound was determined by fluorescence titration of a fixed concentration of peptide with increasing concentrations of lipid. For all peptides the fluorescence signal (intensity or anisotropy) was found to saturate at lipid : peptide ratios greater than 200 : 1.

Interaction of amphipathic peptides with unilamellar bilayer vesicles

Tyrosine exposure probed by second derivative absorption spectroscopy

Ragone et al. (1984) showed that the ratio (*R*) between two peak-to-peak distances in thie second-derivative spectrum of tyrosine-tryptophan mixtures is determined by the polarity of the solvent environment of the tyrosine residues. The ratio is that between the 283 nm minimum and 287 nm maximum peak-to-peak distance and the 290.5 nm minimum and 295 nm maximum peak-to-peak distance.

The *R* values for peptides A, B, D and E that contain a single tyrosine residue at postition 7 are summarised in Table 2. For peptides in solution, the *R* value is essentially

Table 3 Fluorescence quantum yield ratios (relative to tryptophan, pH 7.4) and fluorescence anisotropy values of the 18-residue amphipathic peptides in buffer and in the presence of egg phosphatidylcholine vesicles (lipid/peptide molar ratio 1300 : 1). The excitation wavelength was 295 nm

Peptide (Trp sequence position)	Quantum yield ratios (relative to trp, pH 7.4)		Fluorescence anisotropy (r)	
	Solution (±0.05)	EggPC (±0.05)	Solution (±0.002)	EggPC (±0.002)
A (2)	0.51	0.68	0.033	0.109
B (3)	0.74	0.95	0.039	0.103
C (7)	0.85	1.17	0.045	0.118
D (12)	0.84	0.85	0.040	0.052
E (14)	1.04	0.85	0.042	0.060

independent of the position of the tryptophan. The mean value [0.9 ± 0.04 (SD)] is close to that reported for a model tryptophan-tyrosine mixture (1 : 1 mole ratio) in aqueous solution (0.93; Ragone et al. 1984).

In the presence of unilamellar eggPC vesicles, perturbations are observed in the second-derivative spectra of peptides A, B, D and E and take the form of a decrease in R value to a mean of 0.50 ± 0.07 (SD) (Table 2). The large decrease in R value on binding to lipid suggests that the tyrosine at position 7 of these peptides is located in a nonpolar environment provided by the lipid bilayer.

The R value for peptide C, a peptide that contains no tyrosine, undergoes a slight decrease from 0.70 in solution to 0.64 in the presence of eggPC vesicles. This is consistent with studies that show that the second-derivative spectraum of model tryptophan compounds is only marginally affected by polarity. Ragone et al. (1984) report a mean value for *N*-acetyl-L-tryptophanamide of 0.68 ± 0.02 (SD) in 11 solvents of varying polarity, which compares with our value of 0.67 ± 0.04 (SD) for the single tryptophan residue in peptide C.

Tryptophan fluorescence quantum yield ratios and anisotropies

Interaction of the peptides with a lipid surface was also assessed by examining the tryptophan fluorescence quantum yield ratios and anisotropies of the peptides in the presence and absence of unilamellar phospholipid vesicles. The quantum yield ratios in Table 3 are reported relative to tryptophan in 10 mM Tris, 150 mM NaCl, pH 7.4. In solution, the quantum yield ratios are dependent on the sequence position of tryptophan and tend to increase as the tryptophan is moved towards the C-terminal end of the peptide. On addition of eggPC vesicles, the fluorescence quantum yields of the tryptophan residues in peptides A, B and C (i.e. position 2, 3 and 7) increase by 33%, 28% and 38%, respectively, while that of tryptophan in peptide E (position 14) decreases by 18%. The tryptophan located at position 12 (peptide D) shows essentially no change in fluorescence quantum yield upon binding to vesicles.

Table 4 Sequence dependence of the tryptophan emission maximum for 18-residue amphipathic peptides A–E (excitation wavelength, 295 nm)

Peptide (Trp sequence position)	Emission maximum (buffer, pH 7.4)	Spectral shift ($\Delta\lambda \pm 2$ nm)	
		In methanol relative to buffer	In eggPC relative to buffer
A (2)	353	−13	−12
B (3)	353	−9	−13
C (7)	353	−11	−14
D (12)	354	−8	0
E (14)	350	−3	−6

The anisotropies (Table 3) show a marginal dependence on tryptophan position in peptides in solution with a mean of 0.040 ± 0.003 (SD), similar to reported values for peptides of similar size (O'Neil et al. 1987). In the presence of vesicles, all peptides show an increase in anisotropy, indicating a reduction in the rotational mobility of the indole ring of the tryptophan residue on binding. However, tryptophan at position 12 shows the least change in anisotropy on binding to lipid.

Tryptophan micropolarity, and accessibility to aqueous and lipid-based quenchers

Tryptophan fluorescence wavelength maxima

The fluorescence maximum of tryptophan is known to be sensitive to the polarity of its microenvironment: generally a blue shift in emission signifies decreased polarity. The fluorescence wavelength maximum of the peptides was recorded in Tris buffer, methanol and in the presence of eggPC vesicles in order to determine the micropolarity of the tryptophan residue in each case. The data are summarised in Table 4.

In solution, the fluorescence of peptides A–E consisted of a broad structureless band with maxima in the range 350–354 nm. These values, when compared with the value for *N*-acetyltryptophanamide in water (354 nm), are consistent with the tryptophan residue in all peptides being exposed to the aqueous solvent.

In methanol, a nonpolar α-helix promoting solvent (CD data not shown), the tryptophan emission maxima for peptides A–E were 340, 344, 342, 346 and 347 nm, respectively. These values can be compared with the value of 340 nm for *N*-acetyltryptophanamide in methanol.

In the presence of eggPC bilayer vesicles, the fluorescence maxima of peptides A, B and C underwent a blue shift of 12–14 nm when compared with the peptides in aquous solution. The shift for peptide E was much less (6 nm), while the emission maximum of peptide D showed no change. This suggests that the tryptophan in peptides A, B, C, and E enters a more nonpolar environment while the tryptophan in peptide D remains in an aqueous environment.

Table 5 Exposure (k_q) of tryptophan residues in peptides A–E to acrylamide quencher. The *L* parameter is the ratio of the exposure of the peptide tryptophan to that of *N*-acetyltryptophanamide in the same solvent

Peptide (Trp sequence position)	Peptides in solution		Peptide-lipid complex	
	k_q [a] ($\pm 0.5\ M^{-1}$)	*L* (± 0.02)	k_q [a] ($\pm 0.1\ M^{-1}$)	*L* (± 0.02)
A (2)	5.5	1.0	1.0	0.2
B (3)	4.9	0.8	0.5	0.1
C (7)	3.6	0.6	0.6	0.1
D (12)	3.4	0.6	1.2	0.2
E (14)	3.1	0.5	0.7	0.1

[a] k_q was determined from the slope of the Stern-Volmer plot and the average lifetime measured by frequency domain fluorimetry

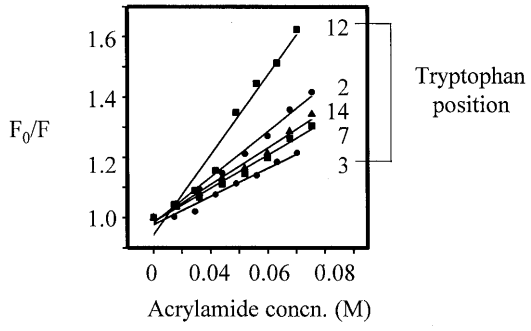

Fig. 3 Stern-Volmer plots of tryptophan fluorescence quenching by acrylamide of peptides A, B, C, D and E in the presence of eggPC vesicles (peptide : lipid mole ratio, 1 : 1300)

Tryptophan quenching by acrylamide

Values of the apparent bimolecular rate constant, $k_{q,app}$, provide an estimate of the relative exposure of tryptophan residues to the aqueous phase (see Methods; Table 5). For peptides in solution, $k_{q,app}$ decreased from 5.5 to 4.9, 3.6, 3.4 and 3.1 M^{-1} for peptides A to E, respectively. In the presence of phospholipid vesicles, the peptides could be divided into three classes based on the Stern-Volmer plots (Figure 3) and the exposure ($k_{q,app}$) of tryptophan residues to the aqueous phase. The tryptophan residue in peptide D was the most exposed, with a value of $k_{q,app}$ of 1.2 $M^{-1}\ ns^{-1}$. Peptides B, C and E had exposure values of 0.5, 0.6 and 0.7 $M^{-1}\ ns^{-1}$, respectively. Peptide A was intermediate between the two extremes with an exposure value of 1.0 $M^{-1}\ ns^{-1}$. These relationships are also reflected in the *L* parameter that expresses the exposure of tryptophan relative to that of *N*-acetyltryptophanamide in aqueous solution (Eftink and Ghiron 1976).

Tryptophan quenching by 5-doxyl stearate

The proximity of tryptophan residues in peptide-lipid complexes to the lipid associated quencher 5-doxyl stearate, which locates the paramagnetic group about 6 Å from the bilayer surface, was examined by comparing quenching efficiencies at a single quencher concentration. Tryptophans at positions 2, 3, 7 and 14 were quenched with similar efficiency [$F_0/F) - 1 = 3.3$, 2.6, 2.7 and 2.9, respectively]. Tryptophan at position 12 was quenched with the least efficiency [$F_0/F) - 1 = 0.8$] and is therefore located further away from the paramagnetic group of the lipid-based quencher.

Correction for reduced diffusion coefficient of the lipid-peptide complex

The collisional quenching of a fluorophore and quencher in free solution is given by:

$$k_q = 4\pi DR$$

where *D* is the sum of the translational diffusion coefficients for the fluorophore and quencher, and *R* is the collision radius approximated as the sum of the molecular radii. Values of k_q for the peptide-acrylamide interaction were calculated using diffusion coefficients estimated according to Johnson and Yguerabide (1985).

The bimolecular rate constant for acrylamide quenching is expected to decrease when the peptide is bound to the comparatively large lipid vesicle owing to the lower translational diffusion coefficient of the peptide-lipid complex. To estimate the magnitude of this effect, we considered a single tryptophan located on a spherical surface of 20 nm diameter. The rate of collisional quenching of the bound fluorophore with the quencher ($k_{q,complex}$) was calculated using the equation of Shoup et al. (1981):

$$k_{q,complex} = 4\pi D_q r (a/\pi r_v)$$

where D_q is the translational diffusion coefficient for the quencher, *r* is the radius of the fluorophore-sphere complex, r_v is the radius of the sphere, and *a* is defined by

$$a = r_v \arccos \{1 - 2[r_f^2/(r_f^2 + r_v^2)]\}$$

where r_f is the radius of the fluorophore. This equation is valid when the area occupied by the fluorophore is small compared to the total surface area of the sphere to which it is attached (the small theta approximation), a situation which is likely to the exist a high lipid to peptide ratios.

The ratio $L (= k_{q,complex}/k_q)$ provides a measure of the expected decrease in the bimolecular rate constant owing to the slower translation diffusion of the peptide-vesicle complex. This theoretical value is 0.41. The experimental values of *L* are listed in Table 5 and are in the range 0.1–0.2.

Discussion

Structure and orientation of the amphipathic peptides on a bilayer surface

The second-derivative absorption spectra of the peptides bound to eggPC vesicles indicate that the tyrosine at posi-

tion 7 is located in a hydrophobic environment, consistent with helical wheel representation in Fig. 1. The values of *R* (Table 2) indicate that the environment experienced by tyrosine is equivalent to that provided by the ethylene glycos (*R* value, 0.48; dielectric constant, 33). Conductance measurements of planar lipid bilayers indicate that the dielectric constant of the acetyl and head group region of the lipid bilayer is in the range 10–40, while that of the hydrocarbon region is as low as 2 (Ashcroft et al. 1980). With the qualification that transbilayer dielectric profile might be perturbed in highly curved bilayers, we suggest that the penetration of the tyrosine residue, and therefore of the helix, into the bilayer is no deeper that the acetyl region of the fatty acid chains. We also note that the decrease in *R* upon formation of the peptide-lipid complex is independent of the position of tryptophan in the sequence (Table 2), implying that the tryptophan substitutions do not influence the position of the tyrosine relative to the bilayer phase.

Tryptophan at position 12 (peptide D)

Several lines of evidence indicate that the tryptophan residue at position 12 (peptide D) is located in a relatively polar environment accessible to quenchers in the aqueous phase.

1. Trp-12 in peptide D showed no change in quantum yield or emission maximum on the binding of the peptide to the lipid surface (Tables 3 and 4).
2. Of all peptides, peptide D showed the smallest increase in steady-state anisotropy on binding to the lipid surface (Table 3), indicating that complex formation resulted in the least restriction of motion of the indole side chain.
3. Trp-12 in the peptide D-lipid complex was most exposed to acrylamide quencher in the aqueous phase (Table 5, Fig. 3).

Tryptophans at positions 3, 7 and 14 (peptides B, C and E)

These tryptophans are in the an apolar environment, as indicated by the substantial blue shift in the emission maximum on binding of the peptides to lipid. The relatively high values of the steady-state anisotropy indicate a restriction in the motion of the indole side chain and/or a change in the limiting anisotropy at infinite time. These residues are buried in the bilayer to an extent that they are the least accessible to (acrylamide) quenching from the aqueous phase, but show the greatest accessibility to (5-doxyl stearate) quenching from the lipid phase. However, attempts to assign relative penetration depths based on the emission maxima of the tryptophans is hampered by the possibility of sequence effects which have been noted previously for other peptide-lipid systems (Jones and Gierasch 1994). These effects become evident when comparing the emission maxima of the tryptophans of the α-helical peptides in methanol with the values obtained for *N*-acetyltryptophanamide in the same solvent. The results show that α-helix formation in methanol results in a red-shift of 7 nm for peptide E, 4 nm for peptide B and 2 nm for peptide C. By correcting the data for the peptide-lipid complexes to account for this effect we obtain *relative* emission maxima of 336 nm for peptide B, 337 nm for peptide C and 337 nm for peptide E. The conclusions reached with regard to λ_{em} (corrected for sequence effects) as an indicator of the polarity of the microenvironment of tryptophan are therefore in agreement with the accessibility data. The emission maxima of tryptophans 3, 7 and 14 indicate that they are located in an environment which is less polar than water (λ_{max} = 354 nm) but not quite as nonpolar as the acyl chain region of the bilayer (λ_{max} = 320–330 nm; Voges et al. 1987), indicating that the nonpolar face of the helix penetrates no deeper than the ester linkages of the phospholipid. This conclusion is therefore in qualitative agreement with the data derived from tyrosine absorption discussed above.

Tryptophan at position 2 (peptide A)

The high degree of quenching by 5-doxyl stearate suggests that the tryptophan in peptide A is closest to the paramagnetic quenching group. The accessibility of tryptophan at position 2 to aqueous phase quencher (acrylamide) is intermediate between that for position 12 and positions 3, 7 and 14. Its anisotropy is high (0.109) and its emission maximum (341 nm) is not quite as blue shifted as that for positions 3 and 7 (340 and 339 nm, respectively). Comparison with the absolute wavelength maximum of the tryptophan at position 14 in peptide E (344 nm) might suggest that the peptide A tryptophan is located in a less polar environment than in peptide E. However, taking into account the sequence/helix effect discussed above, the relative ordering of the wavelength maxima is altered to 340 nm for peptide A and 337 nm for peptide E. The corrected order of tryptophan polarity based on the wavelength maximum is in agreement with the ordering of the tryptophan accessibilities to a quencher in the aqueous phase. Together, the micropolarity and exposure data suggests that the tryptophan residue in the peptide A is located in a more hydrated region of the bilayer than the tryptophan in peptides B, C and E. Although the tryptophan at position 2 is separated from the hydrophilic face of the helix by a lysine residue, it is possible that rotation of the indole about the β-carbon might lead to burial in the head-group region of the lipid with a consequent decrease in the rotational motion of the indole moiety. An alternative explanation is that the peptide hydrophobic-hydrophilic interface lies below the membrane-water interface, thus locating the first few residues of the polar face in the lipid phase. To summarise, the spectral properties of tryptophans at positions 2, 3, 7, 12 and 14 are consistent with the helical wheel orientation of the peptide depicted in Fig. 1.

Translational diffusion of the peptide-lipid complex

Although the spectral parameters indicate that tryptophan 12 is in an aqueous environment, there is a significant decrease in its apparent exposure ($k_{q,app}$) on binding to the lipid surface. The comparison of the theoretical with the experimental bimolecular rate constant (parameter L, Table 5) indicates that much of the decrease can be attributed to (1) the slower translational diffusion of the peptide upon attachment to the much larger vesicle, (2) the small fraction of the vesicle surface area occupied by tryptophan and (3) to a decreased approach angle of the quencher. These factors are partly accommodated by the theory of Shoup et al. (1981). In view of the approximations made in the calculation of the theoretical k_q, a precise figure cannot be given as to the reduction in the reducted diffusion coefficient. However, the calculation demonstrates that most of the reduction in $k_{q,app}$ can be attributed to the decreased diffusion coefficient of the peptide-vesicle complex.

Other possible interpretations

The spectral properties of the tyrosine and tryptophan residues are consistent with the orientation of the helix depicted in Fig. 1. However, the pattern of tryptophan polarity can be supported by an alternative model in which the helices form a transmembrane bundle in which hydrophilic faces of the helices form a central channel. We believe that such a model is unlikely on two grounds. Firstly, the transmembrane model is not supported by data pertaining to the tryptophan exposure unless the hydrophilic channel is completely accessible to acrylamide. Secondly, the data for the quenching by 5-doxyl stearate are not consistent with a transmembrane model in which the efficiency of quenching would depend on the position of the tryptophan in the sequence (Voges et al. 1987). The observed correlation between aqueous exposure/lipid shielding and the polarity of the peptide face in which the tryptophan is located leads to the conclusion that the peptide is aligned parallel to the surface near the interfacial region rather than in a transmembrane orientation.

The environment of the tryptophan residues and the decrease in the ellipticity at 222 nm on peptide binding to lipid are consistent with an α-helical secondary structure. However, the question arises as to whether another secondary structural form, oriented with its long axis parallel to the lipid surface, might also mimic the observed experimental data. Assuming that the tryptophan 12 is fully exposed to the aqueous phase and can therefore be considered an anti-node for the periodic secondary structure function, it is possible to predict the expected polarity pattern for tryptophans at positions 2, 3, 7, 12 and 14 for each of the other major secondary structural forms of a polypeptide chain. The polarity pattern predictions for the β-sheet, 3,10-helix, the π-helix and the α-helix are shown in Table 6 together with the experimentally assigned polarity pattern for the present peptides. Some uncertainty is allowed in the theoretical polarity of residues that might lie close to the polar-nonpolar interface. Local movement of the indole ring with respect to the peptide backbone, movement of the peptide polar-nonpolar interface with respect to the membrane-water interface, and the undefined nature of the polarity of the interfacial region may effect these predictions (designated as NP/P in Table 6). The data show that a periodic structure with 2 residues per turn (the β-sheet) or 4.4 residues per turn (the π-helix) cannot fit the experimental data adequately. The 3,10-helix with 3 residues per turn can reproduce the observed polarity pattern for 4 out of 5 sequence positions but the errant polarity assignment at position 3 cannot be reconciled with the experimental data, which clearly show that position 3 is located in a nonpolar environment. On the other hand, the amphipathic α-helix correctly predicts the polarity pattern for the 5 labelled positions and is therefore seen to provide the best model that fits the experimental data.

Table 6 Effect of secondary structure on the predicted polarity profiles for tryptophan located at positions 2, 3, 7, 12 and 14 and assuming the long axis of the polypeptide lies parallel to the lipid-water interface. P denotes polar positions exposed to aqueous phase. NP denotes non-polar positions and exposed to lipid, and NP/P denotes positions close to lipid-water interface (polarity undefined)

Trp sequence position	Theoretical polarity/secondary structure correlation				Experiment (this work)
	β-sheet	π-helix	3,10-helix	α-helix	
2	P	NP/P	NP	NP/P	NP
3	NP	P	P	NP	NP
7	NP	P	NP	NP	NP
12	P	P	P	P	P
14	P	NP	NP	NP	NP

Comparison with other studies

There are a few studies of peptide-lipid interactions that have employed a fluorescence approach using tryptophan positional isomers. Voges et al. (1987) used single tryptophan alamethicin analogues to prove that the peptide spans the lipid bilayer. In these studies, the value of the emission wavelength maximum of each peptide was qualitatively consistent with the expected orientation of the peptide in the bilayer. These studies used lipid resident quenchers located at defined depths in the bilayer to reveal the relative transmembrane positions of the tryptophan residues in the peptides. Chung et al. (1992) used similar methodologies to study the zero-applied voltage state of model ion channel peptides based on the sequence $(LSSLLSL)_3$. The periodicity in the tryptophan emission maxima and the collisional quenching by cesium ion showed that these peptides oriented with the α-helical axis parallel to the surface. However, these peptides appear to penetrate more deeply into the bilayer than those reported here. For example, analysis of lipid-based quenching indicated that a tryptophan on the nonpolar face of the helix could lie within the region of the phospholipid acyl chains. Moreover, the emission maxima of the tryptophan residues, whether lo-

cated on the polar or nonpolar face of the helix, were more blue shifted than those reported in the present study. The deeper penetration of the $(LSSLLSL)_3$ peptide may reflect its higher average hydrophobicity (+0.52) and is consistent with the observation that an increase in the hydrophobicity of the nonpolar face increases the affinity of the peptide for the bilayer (Kiyota et al. 1996).

The analysis indicates that the class A amphipathic peptides examined here lie parallel to the lipid surface, penetrating no deeper than the carbonyl region of the phospholipid ester groups. Further work is required to understand the factors affecting the degree of penetration and the orientation of amphipathic helices with the membrane surfaces and the associated peptide dynamics.

Acknowledgements This research has been supported by the Australian Research Council. A.H.A.C. is a Postdoctoral Research Fellow of the Australian Research Council.

References

Adler AJ, Greenfield NJ, Fasman GD (1973) Circular dichroism and optical rotatory dispersion of proteins and polypeptides. Methods Enzymol 27: 675–735

Ashcroft RG, Thulborn KR, Smith JR, Coster HGL, Sawyer WH (1980) Perturbations to lipid bilayers by spectroscopic probes as determined by dielectric measurements. Biochim Biophys Acta 602: 299–308

Brasseur R (1991) Differentiation of lipid-associating helices by use of three-dimensional molecular hydrophobicity potential calculations. J Biol Chem 266: 16120–16127

Chakrabartty A, Kortemme T, Oadmanabhan S, Baldwin RL (1993) Aromatic side-chain contribution to far-ultraviolet circular dichroism of helical peptides and its effect on measurement of helix propensities. Biochemistry 32: 5560–5565

Chung LA, Lear JD, De Grado WF (1992) Fluorescence studies of the secondary structure and orientation of a model ion channel peptide in phospholipid vesicles. Biochemistry 31: 6608–6616

Dathe M, Schumann M, Wieprecht T, Winkler A, Beyermann M, Krause E, Matsuzaki K, Murase O, Bienert M (1996) Peptide helicity and membrane surface charge modulate the balance of electrostatic and hydrophobic interactions with lipid bilayers and biological membranes. Biochemistry 35: 12612–12622

De Kroon AIPM, Soekarjo MW, De Gier J, Kruijff de (1990) The role of charge and hydrophobicity in peptide-lipid interaction: a comparative study based on tryptophan fluorescence measurements combined with the use of aqueous and hydrophobic quenchers. Biochemistry 29: 8229–8240

Eftink MR, Ghiron CA (1976) Fluorescence quenching of indole and model micelle systems. J Phys Chem 80: 486–493

Eisenberg D, Wesson M, Wilcox W (1989) Hydrophobic moments as tools for analyzing protein sequences and structures. In: Fasman G (ed) Prediction of protein structure and principles of protein conformation. Plenum Press, New York, pp 635–646

Hefele WJ, Goormarghtigh E, De Meutter J, Ruysschaert JM, Jonas A (1990) Investigation of the lipid domains and apolipoprotein orientation in reconstituted high density lipoprotein by fluorescence and infrared methods. J Biol Chem 265: 20044–20051

Huang HW, Wu Y (1991) Lipid-alamethicin interactions influence alamethicin orientation. Biophys J 60: 1079–1087

Johnson DA, Yguerabide J (1985) Solute accessibility to N-fluorescein isothiocyanate-lysine-23 cobra α-toxin bound to the acetylcholine receptor. Biophys J 48: 949–955

Jones JD, Gierasch LM (1994) Effect of charged residue substitutions on the membrane-interactive properties of signal sequences of the *Escherichia coli* LamB Protein. Biophys J 67: 1534–1545

Kanellis P, Romans A, Johnson BJ, Kercreb H, Chiovetti R, Allen TM, Segrest JP (1980) Studies of synthetic peptide analogues of the amphipathic helix. Effect of charged amino acid residue topography on lipid affinity. J Biol Chem 255: 11464–11474

Kiyota T, Lee S, Sugihara G (1996) Design and synthesis of amphipathic α-helical model peptides with systematically varied hydrophobic-hydrophilic balance and their interaction with lipid and biomembranes. Biochemistry 35: 13196–13204

Mishra VK, Palgunachari MN (1996) Interaction of model class A1, class A2 and class Y amphipathic helical peptides with membranes. Biochemistry 35: 11210–11220

Mishra VK, Palgunachari MN, Segrest JP, Anantharamaiah GM (1994) Interactions of synthetic peptide analogues of the class A amphipathic helix with lipids. Evidence for the snorkel hypothesis. J Biol Chem 269: 7185–7191

Mishra VK, Palgunachari MN, Lund-Katz S, Phillips MC, Segrest JP Anantharamaiah GM (1995) Effect of the arrangement of tandem repeating units of class A amphipathic α-helices on lipid interaction. J Biol Chem 270: 1602–1611

New RRC (1990) Preparation of liposomes. In: New RRC (ed) Liposomes: A practical approach. IRL Press, Oxford, pp 33–104

O'Neil KT, Wolfe HR, Erickson-Viitanen S, Degrado WF (1987) Fluorescence properties of calmodulin-binding peptides reflect alpha-helical periodicity. Science 236: 1454–1456

Ragone R, Colonna G, Balestrieri C, Servillo L, Irace G (1984) Determination of tryrosine exposure in proteins by second-derivative spectroscopy. Biochemistry 23: 1871–1875

Segrest JP, De Loof H, Dohlmar JG, Brouilette CG, Anantharamaiah GM (1990) Amphipathic helix motif: classes and properties. Proteins 8: 103–117

Shon K-J, Kim Y, Colnago LA, Opella SJ (1991) NMR studies of the structure and dynamics of membrane-bound bacteriophage Pf1 coat protein. Science 252: 1303–1305

Shoup D, Lipari G, Szabo A (1981) Diffusion-controlled bimolecular reaction rates: the effect of rotational diffusion and orientational constraints. Biophys J 36: 697–714

Venkatachalapathi YV, Phillips MC, Epand RM, Epand RF, Tyler EM, Segrest JP, Anantharamaiah GM (1993) Effect of end group blockage on the properties of a class A amphipathic helical peptide. Proteins Struct Funct Genet 15: 349–359

Vogel H (1987) Comparison of the conformation and orientation of alamethicin and melittin in lipid membranes. Biochemistry 26: 4562–4572

Voges KP, Jung G, Sawyer WH (1987) Depth-dependant fluorescence quenching of a tryptophan residue located at defined positions on a rigid 21-peptide helix in liposomes. Biochim Biophys Acta 896: 64–76

Wu Y, Huang HW, Olah GA (1990) Method of oriented circular dichroism. Biophys J 57: 797–806